

Effect of buffer gas on an electromagnetically induced transparency in a ladder system using thermal rubidium vapor

Armen Sargsyan and David Sarkisyan

*Institute for Physical Research, National Academy of Sciences, Ashtarak 2, Armenia*Ulrich Krohn,^{*} James Keaveney, and Charles Adams*Department of Physics, Rochester Building, Durham University, South Road, Durham DH1 3LE, United Kingdom*

(Received 23 May 2010; published 25 October 2010)

We report on the observation of electromagnetically induced transparency in a ladder system in the presence of a buffer gas. In particular, we study the $5S_{1/2}$ - $5P_{3/2}$ - $5D_{5/2}$ transition in thermal rubidium vapor with a neon buffer gas at a pressure of 6 Torr. In contrast to the line-narrowing effect of buffer gas on Λ systems, we show that the presence of the buffer gas leads to an additional broadening of (34 ± 5) MHz, which suggests a cross section for Rb($5D_{5/2}$)-Ne of $\sigma_k^{(D)} = (23 \pm 4) \times 10^{-19}$ m². However, in the limit where the coupling Rabi frequency is larger than the collisional dephasing, a strong transparency feature can still be observed.

DOI: [10.1103/PhysRevA.82.045806](https://doi.org/10.1103/PhysRevA.82.045806)

PACS number(s): 42.50.Gy, 34.90.+q

The effect of electromagnetically induced transparency (EIT) arises due to coherence in three-level systems as first described in [1,2] and experimentally demonstrated in [3]. Typically, the three-level system consists of two long-lived states ($|1\rangle$ and $|3\rangle$), which are coupled by two lasers, labeled *probe* and *coupling*, with Rabi frequencies Ω_p and $\Omega_c (> \Omega_p)$, to a radiative state $|2\rangle$ with a lifetime $1/\Gamma_2$.

If the two lasers are resonant, that is, the detunings $\delta_{12} = \delta_{23} = 0$, the imaginary part of the one-photon coherence $\text{Im}(\rho_{12})$ and the absorption coefficient $\alpha \propto \text{Im}(\rho_{12})$ are zero, rendering the medium fully transparent [4]. For $\Omega_p < \Gamma_2$ the transparency is caused by a destructive interference of the excitation amplitudes into the intermediate state $|2\rangle$, which results in the occupation of a dark state $|\emptyset\rangle \simeq |1\rangle$ with no contribution from the radiative state. The width of the transparency window is determined by the dephasing rate between states $|1\rangle$ and $|3\rangle$, Γ_{13} , and can be much narrower than the natural linewidth, $\Gamma_{13} < \Gamma_2$.

For photon-storage applications, one is interested in reducing the dephasing rate as the narrow resonance results in a large group index [5] and enables long photon-storage times [6]. For thermal atoms, the dephasing rate can be reduced by using the hyperfine ground states, as the long-lived states form a Λ system, and a buffer gas to increase the interaction time with the laser beams [7–9].

Another topic of interest is the ladder or cascade system where $|3\rangle$ is a higher energy excited state [10–12]. For example, if state $|3\rangle$ is a Rydberg state [13], this opens interesting possibilities for quantum information [14–16] and electrometry [17,18]. In the ladder system, the dephasing rate is typically larger than for Λ systems due to the spontaneous decay of level $|3\rangle$. Otherwise, EIT in Λ and ladder systems show generally similar properties. However, the addition of a buffer gas changes this behavior dramatically. In Λ systems, the dephasing of the ground-state coherences due to the collisions with the buffer gas is negligible and, instead, the increased transient time due to collisional diffusion allows an

extremely narrow linewidth to be observed [7,19]. In contrast, for cascade systems the collisional dephasing due to the buffer gas becomes the dominant line-broadening mechanism and it is predicted that the EIT threshold (coupling power required to observe a transparency) and linewidth increase monotonically with the buffer-gas pressure [20].

However, as suggested in [20], one still expects to see a transparency effect if the Rabi frequency of the coupling laser is larger than the dephasing rate. In this regime, where $\Omega_c > \Gamma_2$, the medium is rendered transparent by means of Autler-Townes splitting of the resonance, and the transparency effect is no longer dependent on destructive interference. In what follows, the terms *transparency* and *EIT* are used in a broader sense and not restricted to coherent excitation of a dark state. Although EIT in a ladder system in the presence of a buffer gas has not been studied extensively, it remains of interest to study such transparency features especially in submicron cells [21,22]. In this case, the implementation of the EIT effect could be used as a tool to develop quantum information applications or to study the long-range van der Waals atom-surface interaction for cell thicknesses $\ell < 100$ nm.

Although for a ladder system the addition of buffer gas results in increased broadening, in some experimental situations the Rb-Ne collisions might be advantageous. In particular, when the laser spot sizes become small ($\simeq 1$ μm), the transient time broadening in a pure atomic vapor ($\simeq 50$ MHz) exceeds the collisional broadening between the atoms and the buffer gas. In this case, the addition of a buffer gas with a low pressure ($\simeq 1$ Torr) would result in the reduction of the transient time broadening while leading to only a small additional collisional broadening ($\simeq 10$ MHz).

In this article, we demonstrate ladder EIT in Rb thermal vapor in the presence of a buffer gas. We show that for the $5S$ - $5P$ - $5D$ system in Rb vapor and Ne buffer gas (6 Torr), this leads to an additional broadening of (34 ± 5) MHz of the transparency window, which is consistent with a Rb($5D$)-Ne cross section of $\sigma_k^{(D)} = (23 \pm 4) \times 10^{-19}$ m².

A schematic of the experimental setup is shown in Fig. 1. Probe and coupling laser beams are produced by extended cavity diode lasers operating at wavelengths $\lambda_p = 780$ nm

^{*}u.m.krohn@durham.ac.uk

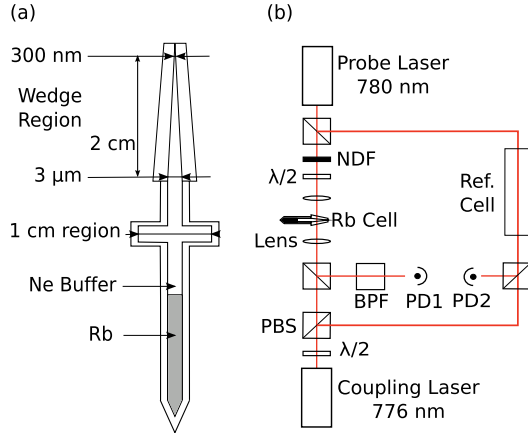


FIG. 1. (Color online) (a) Schematic of the Rb vapor cell. The cell consists of two separate regions: a region with thickness of 10 mm and a wedge, where the thickness varies between 300 nm and 3 μm over a region of approximately 2 cm. (b) Schematic of the experimental setup. A reference cell of length 10 cm is used for frequency calibration. A photodiode PD1 (PD2) is used to record the signal from the buffer cell (reference cell). NDF, neutral density filter; PBS, polarizing beam splitter; BPF, band pass filter; and $\lambda/2$, half-wave plate.

and $\lambda_c = 776$ nm, respectively. The beams counterpropagate through a Rb cell to minimize the Doppler broadening of the transition to the residual Doppler width $\delta\omega_d = |\omega_p - \omega_c| \bar{v}_{\text{Rb}}/c \simeq 2\pi \times 2$ MHz for a temperature of $T = 430$ K and $\bar{v}_{\square} = \sqrt{8k_B T/(\pi m_{\square})}$, where \square is either Rb or Ne. Lenses with a focal length of 20 cm are used to create a spot size ($1/e^2$ diameter, i.e., distance where the power drops to 13.5% of its peak value) in the cell of $d = 27$ μm . The time of flight of the atoms through the beam is $\tau = d/\bar{v} \simeq 80$ ns in a thermal rubidium vapor and, hence, a transient time broadening in the absence of collisions with the buffer gas $\delta\omega_{\tau} = \tau^{-1} \simeq 2\pi \times 2$ MHz. In the presence of the Ne buffer gas, the transient time broadening is reduced by almost three orders of magnitude [23].

In order to calibrate the frequency axis, a part of each beam is directed through a reference Rb vapor cell of length 10 cm. The coupling laser is resonant with the $5P_{3/2} \rightarrow 5D_{5/2}$ ($|2\rangle \rightarrow |3\rangle$) transition, that is, $\delta_c = 0$. The probe laser is scanned across the frequency range of the D_2 line ($|1\rangle \rightarrow |2\rangle$).

Figure 2(a) shows a diagram of the level scheme. Both laser beams have orthogonal linear polarization. A narrow bandpass filter (Semrock LL01-780-12.5) has been mounted in front of PD1 to remove residual 776-nm light on the detector.

The experiments are performed in two cells of similar construction, one pure Rb cell and a Rb buffer gas cell with the addition of $p = 6$ Torr of Ne. The kinetic collision rate between a rubidium atom in the ground state and a neon buffer-gas atom is estimated to be [19]

$$R_k^{(S)} = \frac{P}{k_B T} \sigma_k^{(S)} \bar{v} \simeq 40 \times 10^6 \text{ s}^{-1} \quad (1)$$

for a temperature $T = 430$ K, where k_B is Boltzmann's constant, $\sigma_k^{(S)} \simeq 4 \times 10^{-19} \text{ m}^2$ is the scattering cross section between Rb and Ne in the ground state, and \bar{v} is the average

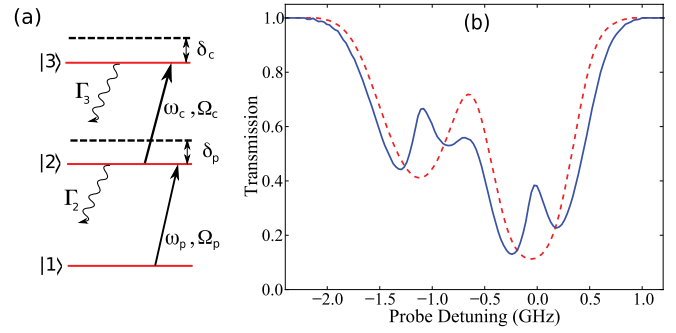


FIG. 2. (Color online) (a) Diagram of the level scheme to clarify the symbols used in the text. (b) Transmission spectra as a function of the probe detuning through the 10-mm buffer gas cell, measured at $T = (52 \pm 1)^\circ\text{C}$ without the coupling beam (dashed red line). The power in the probe beam was $P_p = 1$ μW . The zero of the detuning scale is set to the frequency of the ^{85}Rb $5S_{1/2} F_g = 3 \rightarrow 5P_{3/2} F_e = 4$ transition. The left spectral line corresponds to the ^{87}Rb $5S_{1/2} F_g = 2 \rightarrow 5P_{3/2} F_e = 1, 2, 3$ transition. Switching on the coupling beam (blue line) with a power of $P_c = 196$ mW results in the coupling of F_e to the $5D_{5/2}$ manifold.

relative velocity between Rb and Ne atoms given by $\bar{v} = \sqrt{\bar{v}_{\text{Rb}}^2 + \bar{v}_{\text{Ne}}^2}$.

The mean free path for Rb-Ne collisions is on the order of 10 μm , two orders of magnitude smaller than the mean free path for Rb-Rb collisions (~ 1 mm $\gg \ell$). Thus, in the following discussion Rb-Rb collisions are neglected.

The Rb-Ne collisions lead to a narrowing of the EIT linewidth in a Λ system as the reduction in the transit time broadening dominates over collisional dephasing within the ground-state hyperfine structure. However, in a cascade system, the collisional dephasing between ground and excited states cannot be neglected and leads to a broadening of the EIT linewidth. A typical spectrum of the Doppler-broadened ^{85}Rb and ^{87}Rb transition at a temperature of $(52 \pm 1)^\circ\text{C}$ in the 10-mm buffer gas cell is shown in Fig. 2 (dashed red line). Distinctive transparency peaks appear when the coupling laser is switched on (blue line in Fig. 2) and when the coupling Rabi frequency is sufficiently strong to overcome the collisional dephasing. For the given parameters, the width of the transparency peaks is (105 ± 5) MHz obtained by fitting a Gaussian function to the profiles. Note that no transparency was observed for a cascade system involving highly excited Rydberg states as the coupling laser power was insufficient to fulfill the condition $\Omega_c > \Gamma_{13}$.

For further investigation of the broadening of the transparency feature due to the buffer gas, we focus on the ^{85}Rb feature. The experiments were performed in the wedge region shown in Fig. 1, with the thickness of the atomic sample of order ~ 780 nm to allow tight focusing of the laser beams while still ensuring uniform beam size along the propagation direction. Moreover, we do not observe Dicke narrowing or atom-wall interactions for this cell thickness. Similar experiments with thermal atomic samples of the same size without a buffer-gas background exploiting a Λ system are reported in [24].

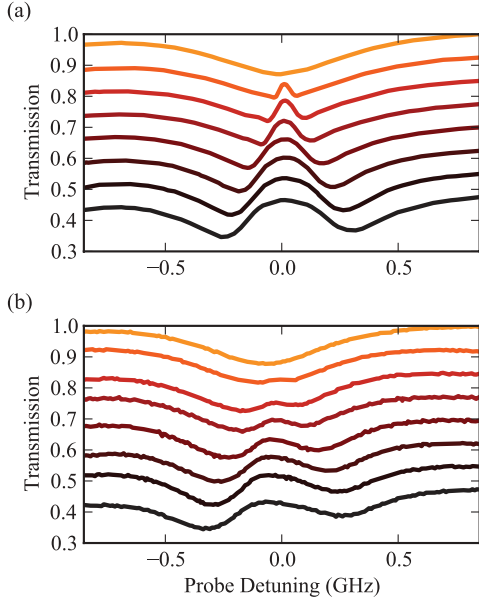


FIG. 3. (Color online) Transmission of the $^{85}\text{Rb } F_g = 3 \rightarrow F_e = 2,3,4$ transitions through the ~ 780 -nm-thick region of the cell, (a) without and (b) with 6-Torr Ne buffer gas, for coupling laser powers of (top to bottom) 0, 4, 14, 28, 70, 112, 154, and 196 mW. The power of the probe laser was $1 \mu\text{W}$, and the temperature of the cell was (430 ± 10) K. An offset in transmission of 0.075 has been added for clarity to all spectra except the topmost.

The spectra in Fig. 3 show the same Autler-Townes splitting of the Doppler broadened resonance as in Fig. 2 both without (a) and with (b) the buffer gas. The additional broadening due to the buffer gas is clearly observed. The width of the transparency feature Γ_{EIT} is obtained by fitting a function of the form $\mathcal{T} \sim 1 - \mathcal{A}_d \exp[-(\Delta^2/(2\delta\omega_d^2))] + \mathcal{A}_{\text{EIT}} \exp[-(\Delta^2/(2\Gamma_{\text{EIT}}^2))]$ to the transmission spectra $\mathcal{T}(\Delta)$. Figure 4 shows the dependence of the transparency linewidth

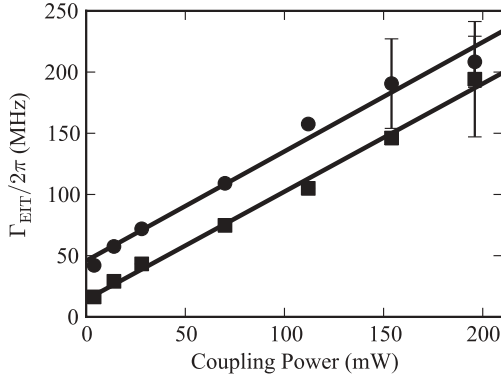


FIG. 4. (Color online) Width of the EIT feature against coupling laser power for the $^{85}\text{Rb } 5S_{1/2} F_g = 3 \rightarrow 5P_{3/2} F_e = 2,3,4 \rightarrow 5D_{5/2}$ transition without (■) and with buffer gas (●), respectively. The widths were obtained by a fit with a Gaussian function to the data shown in Fig. 3. The thickness of the atomic sample is ~ 780 nm. The width shows a linear dependence on the coupling laser power with a slope of (900 ± 50) MHz/W. Adding 6 Torr of Ne buffer gas to the atomic sample results in a EIT linewidth in the low power limit ($P_c \rightarrow 0$) of $2\pi \times (46 \pm 5)$ MHz. Note that the error bars, given by the standard deviation, increase as the Gaussian fit function becomes inaccurate in the Autler-Townes limit.

versus the power of the coupling laser P_c for the measurement with (●) and without (■) buffer gas. This function allows us to quantify the transparency linewidth for low powers ($P_c \lesssim 150$ mW) but shows an increasing deviation for larger powers, as indicated by the error bars in Fig. 4.

The width as a function of the coupling power $P_c \sim \Omega_c^2$ shows a linear dependence as expected from [19]:

$$\Gamma_{\text{EIT}} = \Gamma_{\text{diff}} + \Delta_{\text{EIT}}^c + \frac{\Omega_c^2}{\gamma + \delta_c^2/\gamma}, \quad (2)$$

where

$$\Gamma_{\text{diff}} = \Gamma_{11} + \Gamma_{13} + \Gamma_{31} + \Gamma_{33} \quad (3)$$

is the “diffusion” rate due to the time of flight of the atoms through the laser beam. Note that Γ_{diff} is reduced by $\delta\omega_\tau \simeq 2\pi \times 2\text{MHz}$ due the presence of the buffer gas.

The other rates in (2) are given by

$$\gamma = \frac{1}{2}(\gamma_{21} + \gamma_{23} + \gamma_{2r} + 2\Delta^c) \quad (4)$$

and

$$\Delta^c = \Delta_{11}^c + \Delta_{22}^c - 2\Delta_{12}^c = \Delta_{33}^c + \Delta_{22}^c - 2\Delta_{32}^c, \quad (5)$$

where the Γ_{ij} (collisions) and γ_{ij} (radiative decay) are the incoherent population transfer rates between the states $|i\rangle$ to $|j\rangle$ and Δ_{ij}^c are the collisional-induced decay rates of the respective coherences. State $|r\rangle$ is a reservoir, which considers decay out of the ladder system.

The collisional broadening Δ_{EIT}^c due to collisions between Rb atoms and the buffer gas is

$$\Delta_{\text{EIT}}^c = 2(\Delta_{11}^c + \Delta_{33}^c - 2\Delta_{13}^c). \quad (6)$$

The linear dependence of the width of the transparency resonance on the coupling laser power shows a slope of $\gamma^{-1} \propto 2\pi \times (900 \pm 50)$ MHz/W and an EIT linewidth in the low power limit ($P_c \rightarrow 0$) of $\Gamma_{\text{EIT},0} = 2\pi \times (46 \pm 5)$ MHz due to the presence of the 6-Torr Ne buffer gas. Since the slope γ^{-1} in Eq. (2) is equal within the error bars for the experiments with and without the buffer gas, we conclude that the differential collisional-induced decoherence rate between the ground state $5S_{1/2}$ and the intermediate state $5P_{3/2}$ and between $5P_{3/2}$ and $5D_{5/2}$ is $\Delta^c \simeq 0$, or at least small in comparison to the differential broadening Δ_{EIT}^c between the $5S_{1/2}$ and the $5D_{5/2}$ state.

The linewidth of the EIT feature in the low power limit ($P_c \rightarrow 0$) has the following contributions:

$$\Gamma_{\text{EIT},0} = \delta\omega_d + R_k^{(S)} + R_k^{(D)}. \quad (7)$$

The contribution from the transient time broadening $\delta\omega_\tau$ is negligible in the presence of the buffer gas. Assuming Eq. (1), that is, each collision causes a dephasing and, hence, a linewidth broadening, this indicates that the value for the collisional cross section between the $5D_{5/2}$ state and the neon buffer gas is $\sigma_k^{(D)} = (23 \pm 4) \times 10^{-19}$ m², compared to $\sigma_k^{(S)} \simeq 4 \times 10^{-19}$ m² for the ground state [19]. Note that this calculation neglects collisions between Rb atoms in the $5P$ state and the buffer gas atoms as the population of the $5P$ state is negligible.

In conclusion, we have experimentally shown that a transparency resonance may be observed in a cascade-level scheme in the presence of a buffer gas as long as the coupling field is sufficiently strong such that the Autler-Townes splitting is larger than the collisional dephasing. Furthermore, we have shown that the collisional dephasing due to the buffer gas is five times larger for the excited $5D$ state than the ground $5S$ state.

In future experiments, it might be interesting to study the dependence of the EIT linewidth on the buffer-gas pressure in this ladder system in order to get an accurate value for the collisional cross section $\sigma_k^{(D)}$.

We acknowledge the financial support from the Engineering and Physical Sciences Research Council (EPSRC).

-
- [1] E. Arimondo and G. Orriols, *Lett. Nuovo Cimento* **17**, 333 (1976).
- [2] S. E. Harris, J. E. Field, and A. Imamoglu, *Phys. Rev. Lett.* **64**, 1107 (1990).
- [3] K.-J. Boller, A. Imamolu, and S. E. Harris, *Phys. Rev. Lett.* **66**, 2593 (1991).
- [4] M. Fleischhauer, A. Imamoglu, and J. P. Marangos, *Rev. Mod. Phys.* **77**, 633 (2005).
- [5] C. Liu, Z. Dutton, C. H. Behroozi, and L. V. Hau, *Nature (London)* **409**, 490 (2001).
- [6] U. Schnorrberger, J. D. Thompson, S. Trotzky, R. Pugatch, N. Davidson, S. Kuhr, and I. Bloch, *Phys. Rev. Lett.* **103**, 033003 (2009).
- [7] S. Brandt, A. Nagel, R. Wynands, and D. Meschede, *Phys. Rev. A* **56**, R1063 (1997).
- [8] M. D. Lukin, M. Fleischhauer, A. S. Zibrov, H. G. Robinson, V. L. Velichansky, L. Hollberg, and M. O. Scully, *Phys. Rev. Lett.* **79**, 2959 (1997).
- [9] A. Javan, O. Kocharovskaya, H. Lee, and M. O. Scully, *Phys. Rev. A* **66**, 013805 (2002).
- [10] J. Gea-Banacloche, Y. Q. Li, S. Z. Jin, and M. Xiao, *Phys. Rev. A* **51**, 576 (1995).
- [11] S. Shepherd, D. J. Fulton, and M. H. Dunn, *Phys. Rev. A* **54**, 5394 (1996).
- [12] J. R. Boon, E. Zekou, D. McGloin, and M. H. Dunn, *Phys. Rev. A* **59**, 4675 (1999).
- [13] A. K. Mohapatra, T. R. Jackson, and C. S. Adams, *Phys. Rev. Lett.* **98**, 113003 (2007).
- [14] I. Friedler, D. Petrosyan, M. Fleischhauer, and G. Kurizki, *Phys. Rev. A* **72**, 043803 (2005).
- [15] M. Müller, I. Lesanovsky, H. Weimer, H. P. Büchler, and P. Zoller, *Phys. Rev. Lett.* **102**, 170502 (2009).
- [16] R. Löw and T. Pfau, *Nature Photonics* **3**, 197 (2009).
- [17] A. K. Mohapatra, M. G. Bason, B. Butscher, K. J. Weatherill, and C. S. Adams, *Nature Physics* **4**, 890 (2008).
- [18] M. G. Bason, A. K. Mohapatra, K. J. Weatherill, and C. S. Adams, *Phys. Rev. A* **77**, 032305 (2008).
- [19] M. Erhard and H. Helm, *Phys. Rev. A* **63**, 043813 (2001).
- [20] M. A. Kumar and S. Singh, *Phys. Rev. A* **79**, 063821 (2009).
- [21] M. Fichet, G. Dutier, A. Yarovitsky, P. Todorov, I. Hamdi, I. Maurin, S. Saltiel, D. Sarkisyan, M. Gorza, and D. Bloch, *Europhys. Lett* **77**, 54001 (2007).
- [22] H. Kübler, J. P. Shaffer, T. Baluktsian, R. Löw, and T. Pfau, *Nature Photonics* **4**, 112 (2010).
- [23] R. Wynands and A. Nagel, *Appl. Phys. B* **68**, 1 (1999).
- [24] A. Sargsyan, D. Sarkisyan, and A. Papoyan, *Phys. Rev. A* **73**, 033803 (2006).